Performance Analysis of Distributed Propellers: Efficiency and Noise Trade-Offs in Full-Electric Regional Aircraft

Margalida, G.; Sinnige, T.; de Vries, Reynard ; Exalto, Joaquin; Wolleswinkel, Rob E.

DOI
10.2514/6.2025-3086

Publication date
2025

Document Version
Final published version

Published in
AIAA aviation forum and ASCEND 2025

Citation (APA)
Margalida, G., Sinnige, T., de Vries, R., Exalto, J., & Wolleswinkel, R. E. (2025). Performance Analysis of Distributed Propellers: Efficiency and Noise Trade-Offs in Full-Electric Regional Aircraft. In *AIAA aviation forum and ASCEND 2025* Article AIAA 2025-3688 (AIAA Aviation Forum and ASCEND, 2025). https://doi.org/10.2514/6.2025-3086

AIAA Aviation Forum and ASCEND co-located Conference Proceedings
21 - 25 July 2025, Las Vegas, Nevada
AIAA AVIATION FORUM AND ASCEND 2025

10.2514/6.2025-3086

Performance Analysis of Distributed Propellers: Efficiency and Noise Trade-offs in Full-Electric Regional Aircraft

Gabriel Margalida[1] and Tomas Sinnige[2]
Delft University of Technology, Delft, 2629 HS, The Netherland

Reynard de Vries[3], Joaquin Exalto[4] and Rob E. Wolleswinkel[5]
Elysian Aircraft, Rendementsweg 2, 3641SK Mijdrecht, The Netherlands

Distributed propulsion systems, characterized by multiple propellers, represent a promising approach for full-electric aircrafts, offering several advantages but also introducing technical challenges. The main objective of this paper is to quantify how the propeller performance and noise emissions of an eight-propeller full-electric aircraft configuration compare to that of a conventional fuel-based turboprop. In both cases, the key parameters driving the trade-off between noise emissions and aerodynamic performances are analysed as well as the benefits of each configuration. The propeller noise emissions are analysed in terms of the perceived noise emissions at the three certification points: approach, take-off, and flyover. Optimizations are performed as a function of blade count to investigate the performance and noise trends for different propeller configurations. The results show a promising performance for the battery-electric aircraft with distributed propulsion, achieving a propeller efficiency between 83% and 88% in cruise without incurring a major noise penalty compared to the reference turboprop aircraft, despite the large increase in aircraft size and weight.

Nomenclature

β = Blade pitch angle (°)
BPF = Blade passing frequency
c_i/ceq_i = Equality/inequality constraint
$c_{in.}/c_{out.}$ = Mean chord length inboard/outboard
D = Propeller diameter
C_T = Thrust coefficient, $T/(\rho.f_P^2.D^4)$
C_P = Power coefficient, $T/(\rho.f_P^3.D^5)$
J = Advance ratio, $U_\infty/(2.f_P.R_P)$
f_P = Propeller rotational frequency
η = Propeller efficiency
f = Objective function
f_{out} = Objective function optimum value
γ = Twist angle (°)
M = Mach number
t_j = Duration ratio
Q = Torque (Nm)
R_p = Propeller radius (m)
T = Thrust (N)
U_∞ = Freestream velocity ($m.s^{-1}$)
x_i = Optimization input vector
xl_i / xu_i = Input vector lower/upper bounds
x_{out} = Output optimized vector

[1] Research Associate, Faculty of Aerospace Engineering, Flight Performance and Propulsion
[2] Assistant professor, Faculty of Aerospace Engineering, Flight Performance and Propulsion, AIAA member
[3] Chief Engineer, reynard@elysianaircraft.com, Senior AIAA member.
[4] Aircraft Design & Performance Engineer, joaquin@elysianaircraft.com, AIAA member.
[5] Co-CEO and CTO, rob@elysianaircraft.com, Senior AIAA member.

I. Introduction

Due to the escalating impacts of climate change, the aviation industry faces increasing societal pressure to reduce its environmental footprint. Consequently, stricter regulations and growing demand for sustainable technologies have paved the way of a wave of innovation, with new aircraft concepts emerging regularly. While full-electric aircraft are at the forefront of these initiatives, most designs target Urban Air Mobility (UAM) or general aviation, leaving the regional market—a significant contributor to CO_2 emissions for flights under 2,000 km—largely unaddressed. Regional aviation accounts for approximately 40% of total aviation CO_2 emissions [1], yet the few electric aircraft concepts in this space often compromise on passenger capacity (10 to 30 seats), offer limited ranges easily covered by rail, or rely on alternative solutions such as hydrogen-electric propulsion, hybrid-electric powertrain, or Sustainable Aviation Fuels (SAFs) for longer routes.

Distributed propulsion systems, characterized by multiple propellers (more than 3 per wing), represent a promising approach for full-electric aircraft, offering several key advantages. By distributing thrust across multiple smaller propellers, lower disk loading can be achieved, which can improve propulsive efficiency. It also provides redundancy, reducing the impact of an engine failure on the overall performance, hence reducing the necessary margin for off-design operations. However, those specific configurations technical challenges. Full-electric aircraft are heavier than fuel-based conventional turboprop for similar range and passenger capacity [2], thus increasing the required amount of thrust, and the associated noise emission. The use of multiple propellers also multiplies the number of noise sources. Balancing these trade-offs is critical for assessing the potential of distributed propulsion in full-electric aircraft. The Elysian E9X concept presented in Ref. [1], with its eight-propeller architecture and full-electric design, serves as an ideal case study to explore these issues. The E9X aims to propose a competitive full-electric alternative to regional turboprops and narrow-body turbojets both in terms of range (up to 800km) and passenger capacity (90 PAX). One of the identified design challenges is to design quiet propeller while maintaining high efficiency. This paper focuses on the propeller design of the E9X, specifically assessing these two aspects.

On the one hand, the noise level must comply with the ICAO standards, and ideally perform much better than those requirements to anticipate more stringent regulation. The main noise sources of an aircraft are the engines (jet engines or propellers) and the airframe. During take-off and climb, engine noise is dominant, while airframe noise becomes more significant as speed increases or when landing gears and flaps are deployed. Given the unique configuration of the E9X, quantifying and mitigating noise emissions of the propellers is thus critical to its acceptance. On the other hand, the propulsion system must provide sufficient thrust during the critical phases of the flight, such as take-off and climb while achieving high aerodynamic efficiency to ensure that the aircraft's range is not compromised. Those two parameters, thrust and efficiency, are crucial for the operational viability of the E9X concept.

The main objective of this paper is to compare how the propeller performance and noise emissions of an eight-propeller full-electric configuration compare to the propulsion of a conventional fuel-based and how it translates into the operability of the aircraft. In both cases, the key parameters driving the trade-off between noise emissions and aerodynamic performances will be analysed as well as the benefits of each configuration. The propeller noise emissions are analysed in terms of the perceived noise emissions at the three certification points: approach, takeoff, and flyover. Optimizations are performed as a function of blade count and other propeller design parameters to investigate the performance and noise trends for different propeller configurations. The results show a promising performance for the battery-electric aircraft with distributed propulsion, by not incurring a major noise penalty compared to the reference turboprop aircraft despite the large increase in aircraft size and weight.

II. Methodology and setup

To assess how the propulsion system of an eight-propeller full-electric aircraft compares to a conventional twin fuel-based turboprop, a series of propeller optimizations are conducted for both configurations using a low-fidelity optimization framework developed at TU Delft.

A. Study procedure

The baseline propeller for this study is the TUD-XPROP propeller, originally designed for a regional turboprop with similar specifications to the ATR42/72 family. This propeller is then optimized over a generic flight profile, representing a typical mission, including 3 phases, take-off, climb and cruise, as depicted in Fig. 1.(b). The descent

phase of the flight has been ignored for this study because this phase is not critical nor constraining from a propulsion standpoint and doesn't bring valuable information in the comparison. However, for the assessment of the acoustic emissions, the approach is included because it is part of the certification points.

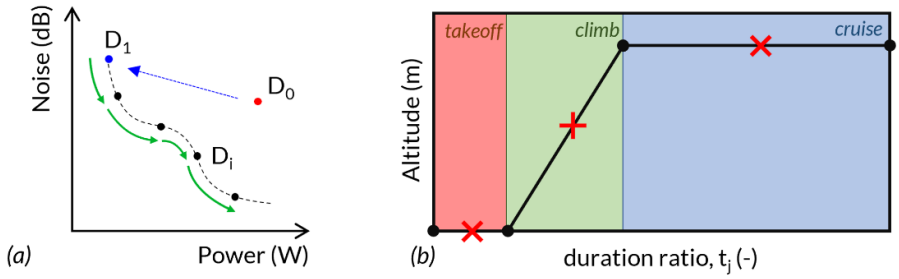

Fig. 1 Optimization methodology. Pareto front generation (a), flight profile example (b)

The noise and aerodynamic objectives are, by definition, conflicting, and they have been treated sequentially as single objective problems using a gradient-based method (SQP algorithm). One objective is optimized while the other is constrained (ε-method). For this study, the propeller is first optimized to minimize the aerodynamic objective (D_0 to D_1 on Fig. 1.(a)), at the expense of the noise performances. A Pareto front is then generated through several consecutive optimizations (D_1 to D_i on Fig. 1.(a)), where the noise is minimized while the aerodynamic objective is constrained to the previous design value with an additional penalty. Using this methodology, Pareto front of optimal design are generated for different sets of parameters (different number of parameters, different number of blades, …) and these designs can then be compared between both configurations.

The optimization workflow is articulated around several modules embedded in a global tool which makes the link from one solver to the other. This workflow, schematized in Fig. 2, includes:

i. a blade designer, using a stack of 2D airfoils to generate a 3D blade. Each section is defined by a set of parameters controlled by several Bézier curves describing their distribution along the blade span.

ii. a propeller/wake generator (geometrical and operational) to define the propeller and its semi-free wake [3].

iii. an aerodynamic solver based on a modern implementation of the Lifting Line Theory [4] (LLT) with several corrections [5], [6], to evaluate the blade local aerodynamic forces and consequently the performances of the propeller (Thrust/Torque).

iv. an acoustic solver, subdivided into 3 modules. A propeller tonal noise module, developed by Goyal [7], based on Hanson's Helicoidal Surface Theory

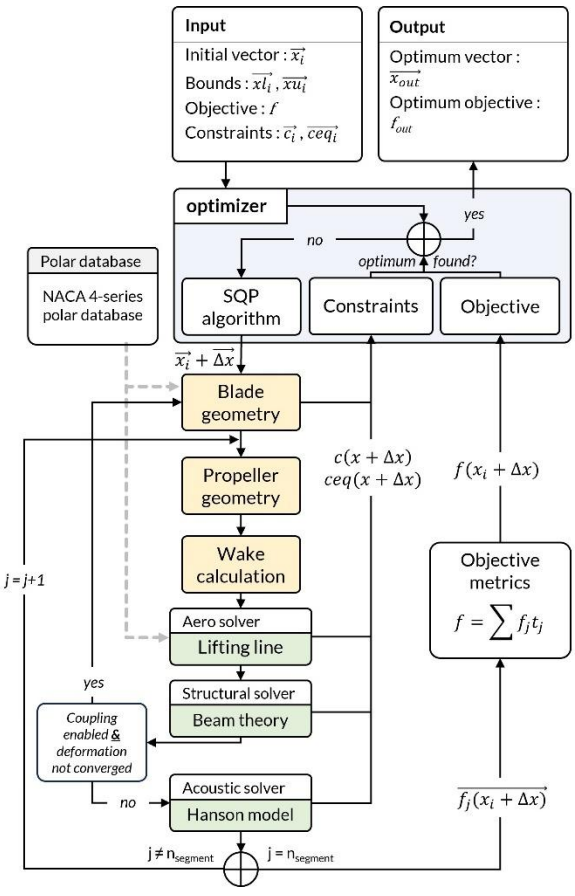

Fig. 2 Optimization workflow

(HST) [8] to evaluate the noise directivity level of the harmonics, a propeller broadband noise module based on the BPM model [9] to estimate the broadband noise generated by the blades and an airframe noise module to estimate the noise of the wings, landing gears and flaps based on Fink's model [10], [11].

v. a structural solver based on Euler-Bernoulli Beam Theory (EBBT) [12] to evaluate the blade stress, deflection, and torsion.

The blade geometry is altered by a set of Bézier curves controlling the distribution of any geometrical parameter along the span through 4 points (P_0 to P_3). The propeller is described by the number of blades, the hub and tip radius R_h and R_t and two operational conditions, the rotational speed **ω** and the pitch setting **β**.

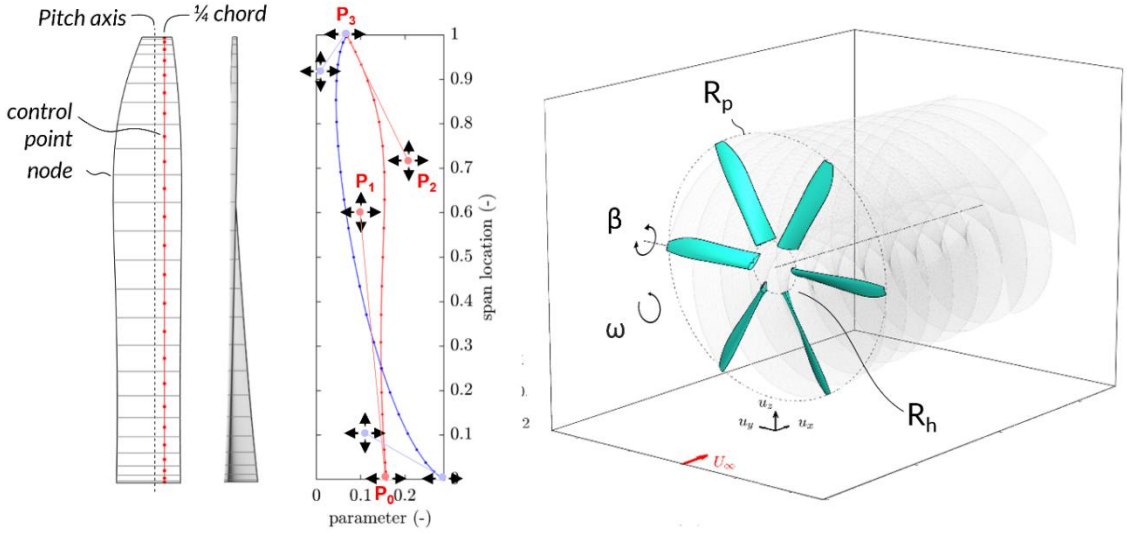

Fig. 3 Blade and propeller parametrization

B. Test case

This study evaluates two distinct aircraft configurations designed for the same mission in terms of range and payload capacity, ensuring a consistent baseline for comparison. The first configuration, referred to as E9X, represents the Elysian E9X full-electric aircraft with distributed propulsion, featuring eight propellers and a maximum takeoff mass (MTOM) of 75 tonnes. The second configuration, referred to as the REF aircraft, is a conventional fuel-based turboprop similar to the ATR72, with two propellers and a MTOM of 25 tonnes. A side-by-side view of both configuration is visible in Fig. 4.

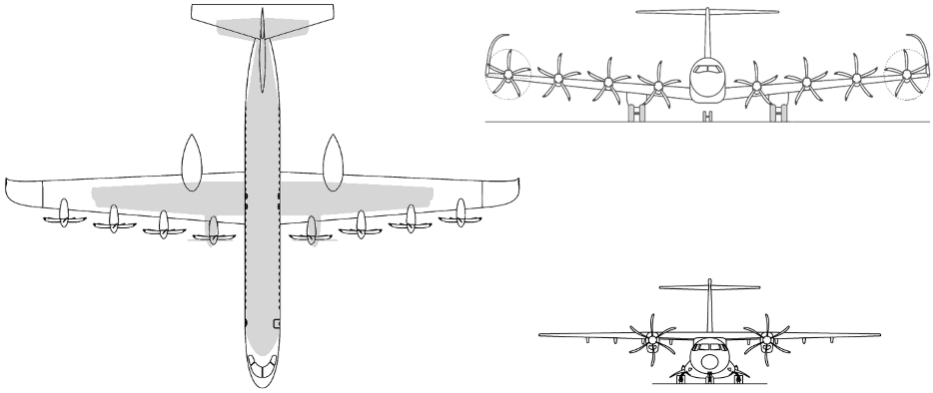

Fig. 4 E9X (left and top right) and REF (bottom right) airframe comparison

As explained in the previous section, the analysis is structured around three key flight phases: takeoff, climb, and cruise. Each phase is characterized by specific operational requirements, including aircraft speed and thrust, reflecting each configuration. For a given phase, the requirements are integrated over time to obtain a single set of parameters used for the optimization. A summary of some key features of both configurations is proposed in Table 1.

	E9X	REF
MTOM (t)	75	25
Wingspan (m)	42	27
L/D (cruise)	23	18
Number of propellers (-)	8	2
Propeller diameter (m)	3.7	4.06

Table 1 Test cases key features.

C. Aerodynamic metric

The driving parameter in the propeller optimization is the total energy consumption for a given flight profile. The higher the propulsive efficiency, the lower the energy consumption. To track this, we can use the averaged shaft power for each phase of the flight and multiply it by the time spent in that phase. This energy consumption can then be linked to the battery weight which will affect the aircraft range. Thus, the total energy consumption will be mainly driven by the climb and cruise phases, which represent most of the flight, while takeoff, which requires a large amount of power for a very short period of time will have little effect on the final value.

However, takeoff propulsive efficiency also has an impact on the maximum required shaft power and torque and thus influences the weight of the powertrain. To account for that effect, an additional weighting is used with a battery-to-aircraft weight ratio for climb and cruise and powertrain-to-aircraft weight ratio for takeoff.

The final aerodynamic metric is defined in Eq. 1.

$$f_{aero} = \frac{m_{energy}}{m_{tot}}\left(\frac{P_{CL}\cdot t_{CL} + P_{CR}\cdot t_{CR}}{E_{tot}}\right) + \frac{m_{engine}}{m_{tot}}\left(\frac{P_{TO}}{P_{\mathrm{TO}}^{\mathrm{init}}}\right) \quad \text{Eq. 1}$$

where subscripts $_{TO}$, $_{CL}$ and $_{CR}$ designate respectively takeoff, climb and cruise, with t is the time spend in a given phase, P the shaft power, m_{tot} the aircraft total mass, m_{energy} the mass of the battery and m_{engine} the mass of the powertrain, E_{tot} the theorical energy consumed in climb and cruise by one propeller (based on the total available energy divided by the number of propeller and accounting for powertrain efficiencies).

D. Noise metric

The noise metric used for this analysis is the Effective Perceived Noise Level (EPNL) as defined by ICAO noise standards. This metric is defined as the sum of the EPNL values computed over three noise signals recorded for three procedures and microphone locations, M1 in takeoff, M2 in flyover and M3 during approach. More details about the flight procedures and the different steps to compute the EPNL can be found in the Appendix 2 of Annex 16 Volume 1 [13]. The calculation process is briefly described in Fig. 5.

The main optimization is done on a flight profile including take-off, climb and cruise. Therefore, only the EPNL in take-off is optimized. The noise metric f_{noise} used for these calculations is thus given by Eq. 2.

$$f_{noise} = EPNL_{M1} \quad \text{Eq. 2}$$

Once the different designs are generated, a detailed analysis of the noise is done for each of the three procedures required by the ICAO noise standard.

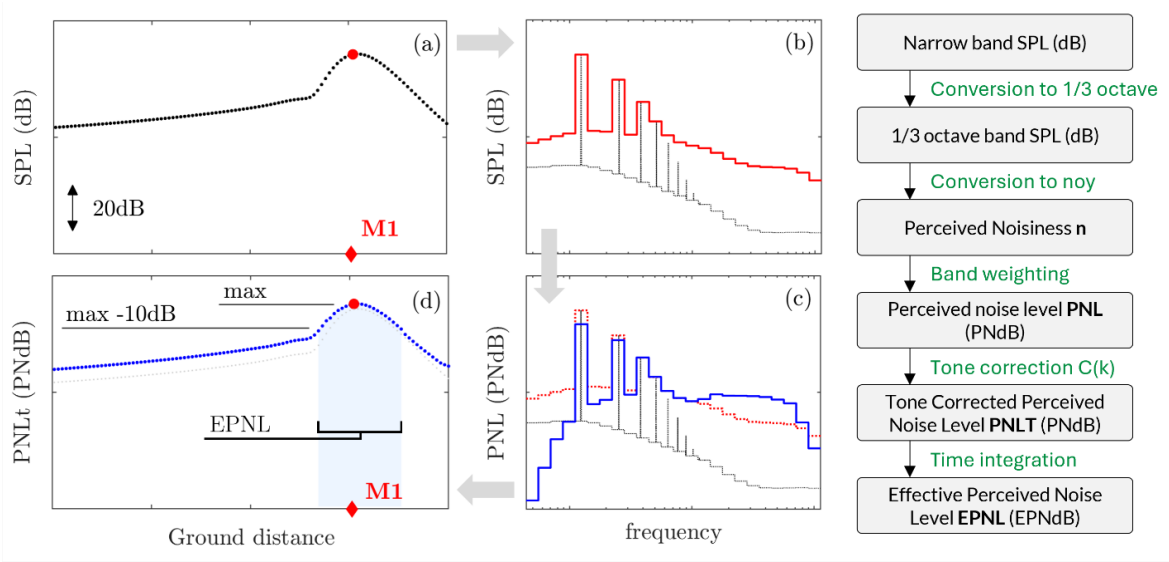

Fig. 5 EPNL calculation procedure. Time history of the SPL (a), spectral shape of the narrow band (black) and 1/3 octave band (red) SPL at a given time (b), spectral shape of the PNL (blue) at a given time (c), time history of the PNL (d)

III. Results

As stated in the previous section, the performances of the propellers optimized for the E9X and for a REF aircraft are compared. To this end, two sets of optimizations have been done using the conditions specific to each aircraft but using the same methodology. An additional blade has been manually defined to match the Hamilton Standard 568F propeller blade.

A. REF propeller optimization

Unlike the E9X, the REF uses combustion engines thus has a more limited operating range. As defined by the FCOM, the nominal rotational speed is set at 100%.Np in take-off, or 1200RPM, and 82%.Np in climb and cruise, or 984RPM. During approach, the lowest rotational speed is used as standard, but the pilot can use the higher one if more deceleration is required.

Therefore, only the pitch and the blade geometry (chord and thickness distributions) are changed during this optimization. The value of the nominal speed, Np, could have been optimized too, but it was intentionally kept constant to represent what is currently used in modern turboprop. The results are displayed in Fig. 6. In addition to the optimized geometries, a blade manually defined to match the HS568F propeller blade of the ATR72 has been computed. The performances of this blade, referred as Dm, are also displayed for comparison.

Without surprise, the overall noise reduction range is small, around -2dB. The manually designed blade displays similar performances, in term of objective metrics, but is slightly louder. This difference comes from the fact that it is significantly thicker than the optimized counterparts, most likely because the structural constraint of the real blade are more stringent than the one set in the optimizer. It can be also seen that a similar sweep angle has been adopted by the optimizer at the blade tip across all designs. For design D3, sweep was constrained at the hub to impose a straighter shape in the inner portion, but the optimizer still favoured a more aggressive sweep distribution compared to the real geometry.

To evaluate the results obtained with the tool, the noise footprint of blade design D_m, matching the HS568F, and the EPNL values have been analysed. The EPNL in each procedure is represented in Fig. 7. The background gradients represent the EPNL as a function of the pitch setting and the rotational speed while the required thrust setting is represented by the red isoline.

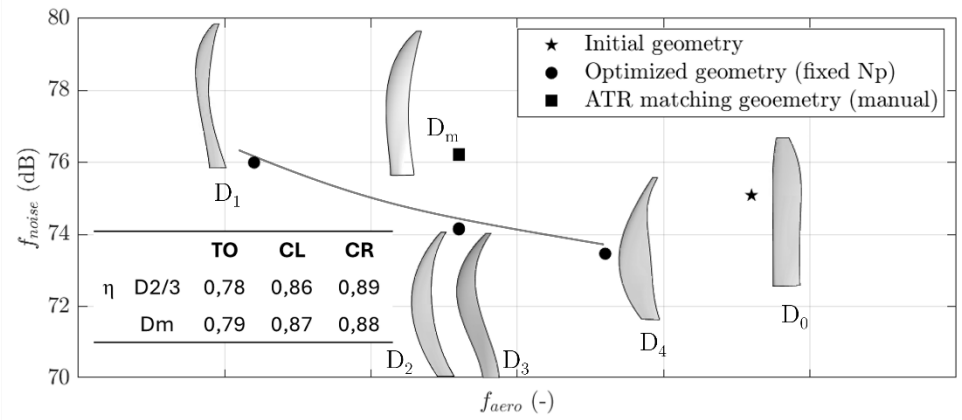

Fig. 6 REF propeller blade optimization results

For each procedure, the correct pitch and rotational speed is selected to ensure that the required thrust setting is satisfied. Using those conditions, the final EPNL can be computed, and is displayed in Fig. 7.(d) with real EPNL values extracted from open access certification data of ATR72 aircraft. An additional error margin has been added to represent the uncertainty induced by the different configurations (MTOM, engine, propeller, …).

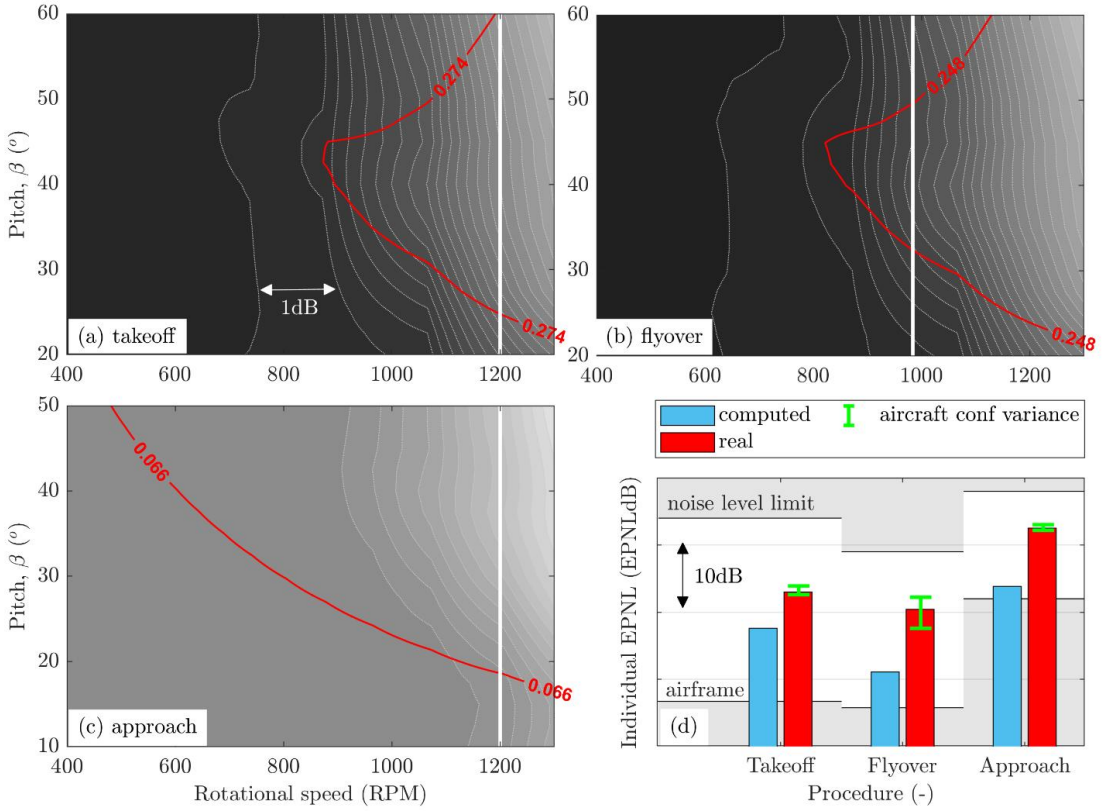

Fig. 7 REF configuration EPNL maps and final EPNL. EPNL map in takeoff (a), flyover (b) and approach (c), and EPNL comparison with real EPNL values extracted from open access certification data

In take-off, the computed and real EPNL value show reasonably good agreement. This procedure is the one with the least uncertainty of the three. Indeed, the vertical distance between the microphone and the flight path is fixed (i.e. 650m) and flight operational conditions are given in the FCOM. In flyover and approach however, the discrepancy is slightly more pronounced. In flyover, the difference as been attributed to the flight path uncertainty because for this

procedure, the microphone ground location is fixed, and the EPNL highly sensitive to the aircraft attitude. In approach, the aircraft altitude with respect to the microphone is also fixed. Here, the difference can be attributed to an incorrect thrust setting, thus underestimating the propeller noise, or to an incorrect airframe noise prediction, leading to an underestimation of the airframe noise.

Despite the discrepancies obtained in flyover and approach, the results obtained for the blade shape and the EPNL during takeoff give us confidence in the overall prediction of the tools used for this study. Indeed, the final EPNL score is highly sensitive to the uncertainties of the input parameters, such as required shaft power, aircraft altitude, aircraft speed, and those uncertainties could explain the difference obtained in those procedures.

B. E9X propeller performance

Several propeller designs have been generated using the optimization methodology described in the previous sections for different number of blades. Some of those designs are displayed in Fig. 8.

Unlike the REF aircraft, the rotational speed is here changed, which translates in a bigger noise reduction range, around -12dB from the most efficient design (upper left of the pareto front) to the quietest (bottom right). To visualize how much noise reduction can be attributed to operational conditions alone (and geometry respectively), two secondary pareto fronts have been generated from design A5/A6 using only the rotational speed and the pitch setting. It can thus be seen that changing the geometry give access to around -4dB additional noise reduction.

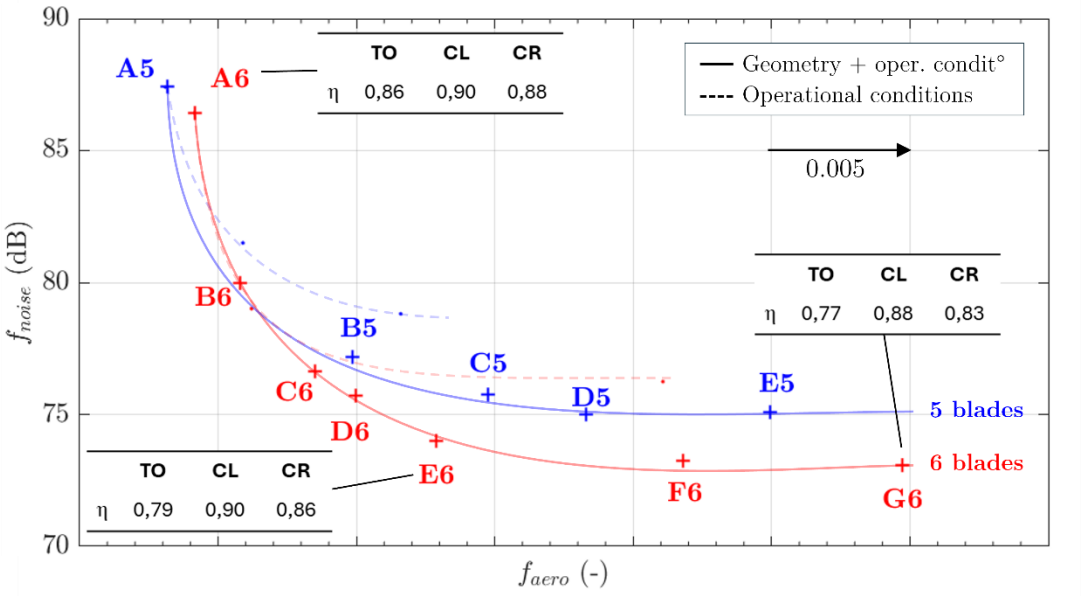

Fig. 8 E9X propeller blade optimization results

From the efficiency standpoint, both climb and cruise exhibit high efficiencies. The geometry is optimized in a way to keep climb and cruise efficiency as high as possible because the optimizer tries to reduce the EPNL in takeoff. Similarly to the REF, the shaft power is around 50% higher in climb than in cruise, but the climb duration (compared to cruise) is much longer for the E9X. This leads to a similar energy requirement in climb and cruise for the E9X. It is thus more beneficial to optimize this phase. In addition, the E9X propellers operate under lower loads and exhibit a lower torque thanks to the distributed propulsion architecture, leading to a higher efficiency

In cruise however, the higher speed in cruise (185m.s-1 compared to 123m.s-1 for the average climb), leads to a higher helical tip Mach number and a larger portion of the blade operating above Mach 0.7, where compressibility effects start to appear. This translates as a result in higher aerodynamic losses and higher torque, and thus a lower efficiency overall.

It has been decided during the project to go for quieter propeller design, and design E6 was selected as a good trade-off between noise and efficiency. Similarly to the REF configuration, the EPNL maps of the E9X design E6 is represented in Fig. 9. In addition to the thrust requirement isoline, the maximum allowable stress isoline is displayed in green. This constraint has been set to 50% of the Yield Strength of the material used for the blade. Unlike the REF propeller, the rotational speed can be freely changed in each procedure, giving a wide range of conditions, going from high rotational speed and low pitch to low rotational speed and higher pitch.

To explore how the EPNL varies, two specific cases are analysed: $E6_{high}$ and $E6_{low,}$ respectively corresponding to efficient operations and quiet operations. For a fixed thrust setting, a large range of operational conditions can thus be used during the different phases of the flight. This flexibility is specifically possible in the case of the E9X because its propellers are supposed to be powered by electric motors. This allows to tune the noise perceived from the ground in a range of around 9dB at the expanse of around 10% and 7% decrease in efficiency during take-off and flyover respectively. Most importantly, this tuning can be adapted to each specific case (conditions, mission profile, airport localization, local noise regulation, …), and doesn't account for any gain that propeller synchrophasing could grant.

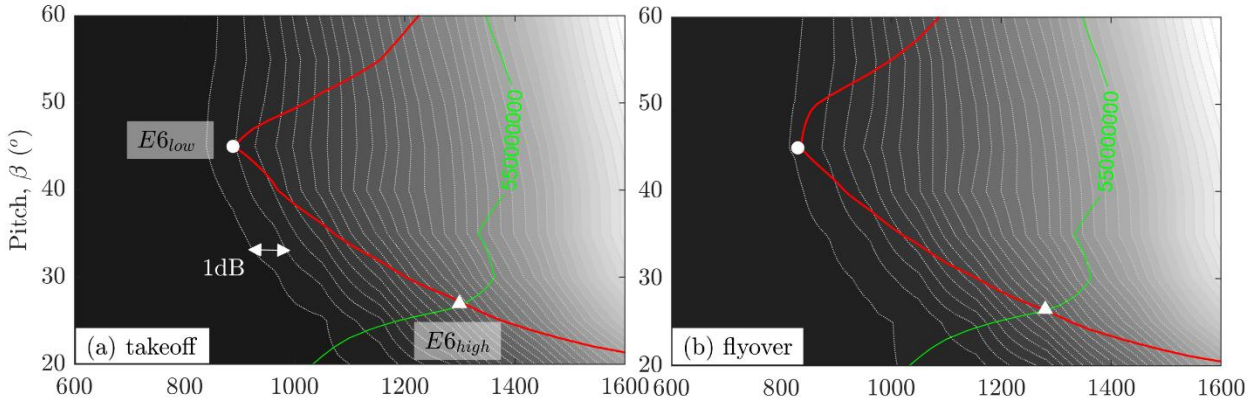

Fig. 9 E9X configuration EPNL maps

The evolution of the overall perceived noise level over time and the contribution of each noise sources has then be analyzed for both $E6_{high}$ and $E6_{low}$. Those results are displayed in Fig. 10. In take-off and flyover, Fig. 10(a).(d).(g) and Fig. 10(b).(e).(h) respectively, propeller noise goes from a dominant contribution for efficient operations, where the entire integration duration is dominated by the tonal noise, to a much lower footprint during quiet operations where airframe and flaps noise dominate. The impact on the final EPNL value is significant: for $E6_{high}$, around 85% and 75% of the EPNL, in take-off and flyover respectively, is due to the propeller tonal noise, while for $E6_{low}$, it would account for around 15% and 0% of the final EPNL. In approach however, propeller tonal noise is significantly lower than airframe noise (airframe, flaps and landing gears). For this specific procedure, propeller noise isn't much of a problem, but airframe is instead.

These results are very promising from a propeller noise perspective, as the noise can be reduced to a negligible level compared to other sources (i.e. airframe noise). However, they also highlight the significant impact of the airframe noise in the case of the E9X. It is thus clear that for a given propeller geometry, the noise footprint can greatly change with the operational conditions used. Lowering the propeller efficiency by reducing the rotational speed gives access to low noise operations where propeller noise disappears under the airframe noise. When noise reduction isn't required, rotational speed can be increased to operate at higher efficiency.

This also implies that an optimum must be found between the two cases (i.e. short and loud or long and smooth). As the propeller tonal noise decreases, airframe noise contributes progressively more to the final EPNL.

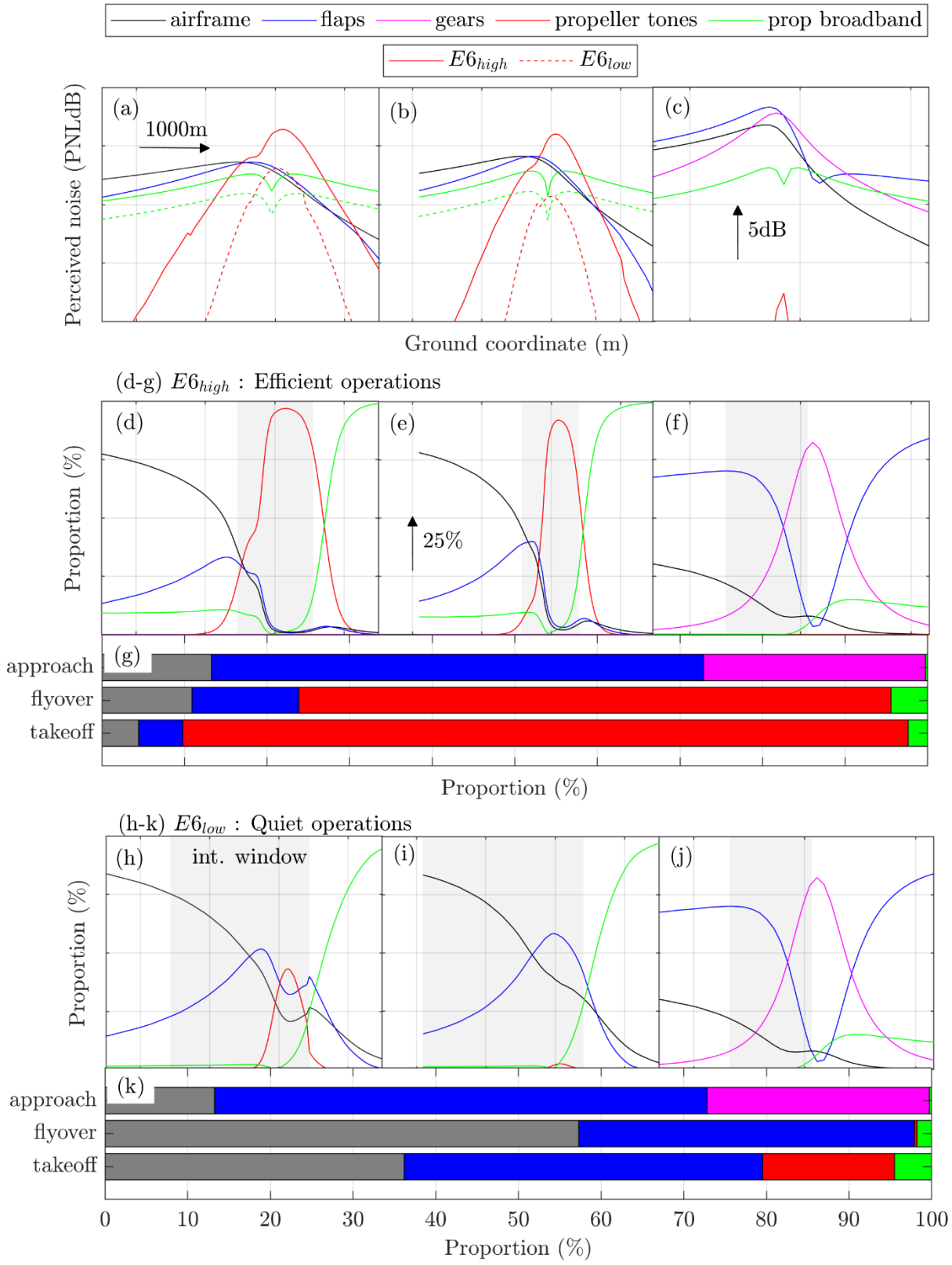

Fig. 10 Individual noise sources contributions to the perceived noise level. Perceived noise in takeoff/flyover/approach (left to right), proportion of each sources for the $E6_{high}$ case (d-f) and total contribution (g), proportion of each sources for the $E6_{low}$ case (g-i) and total contribution (k)

C. E9X and REF performances comparison

In the previous sections, the noise emissions of each configuration, E9X (design E6) and REF (design Dm), have been analyzed individually. In Fig. 11 and Table 2, the EPNL in takeoff and the efficiencies of several propeller designs for the E9X have been compared to the computed propeller for the REF and to the real EPNL data of the ATR72 and A320.

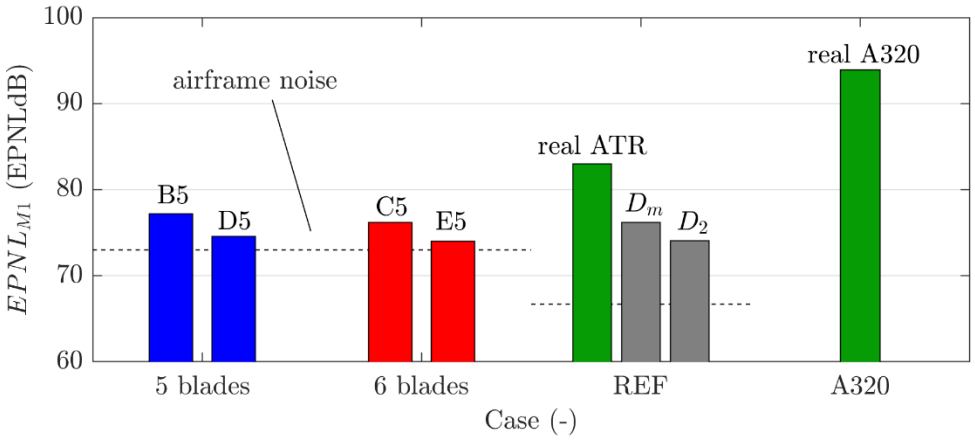

Fig. 11 EPNL during takeoff for computed and real cases

As it can be seen in Fig. 11, for the E9X, regardless of the propeller design (A5/6 excluded), the EPNL score falls in the same range as the optimized propeller D2 or the manually designed blade Dm. It is also clearly visible in this comparison how the propeller noise compares to the airframe noise in both cases. Indeed, for the quietest E9X designs, the takeoff EPNL score is very close to the limit set by the airframe noise, while still largely dominated by propeller noise for the REF case. From the REF case Dm to the selected design E6 for the E9X, the airframe noise adds more than 6dB to the EPNL in takeoff but the final scores are similar. It should be also noted that the computed noise of the E9X is significantly lower than the A320 while having a similar airframe size.

	Takeoff	Climb	Cruise
E6	0,79	0,90	0,86
D_m	0,79	0,87	0,89

Table 2 E9X and REF propeller efficiencies

In term of aerodynamic performances, both configurations exhibit similar efficiencies. The main difference, already discussed in the previous sections, is found in the phase that exhibit the highest efficiency. Indeed, for the REF case, the highest efficiency is in cruise, because most of the flight duration is spent in this phase. For the E9X, it is in climb. Indeed, in cruise, the aircraft speed is higher than the REF and compressibility effects starts to appear. In climb, the 8 propellers leads to lower blade loading and lower torque, hence better efficiency.

IV. Conclusions

The objectives of this study were to generate several propeller designs with different aerodynamic and noise trade-off, to estimate the EPNL of selected designs and to compare those designs to a propeller optimized using the REF conditions.

More specifically, the goal of the analysis was to : (i) evaluate the tradeoff between noise and efficiency for the E9X; (ii) to estimate the noise of some of the designs using the noise certification standard procedure; and (iii) to compare the performances of the E9X selected propeller design to a propeller configured for the current generation of turboprops, such as the ATR72.

Reducing propeller noise can be achieved by reducing the rotational speed, which is a particularly accessible option with electric engines, at the cost of lower propeller efficiency. A range of 10EPNLdb reduction for a loss of 10% in efficiency, and vice-versa, has been achieved. A large portion of the noise reduction obtained during the optimization is primarily due to the rotational speed reduction (lower tip Mach number, lower frequency). Further reduction can be obtained by changing the blade geometry (chord, sweep, …) to access lower rotational speeds. In the tested configurations, the 6-bladed propellers result in lower noise levels at the cost of a smaller efficiency penalty compared to the 5-bladed case. Therefore, increasing the number of blades even more to further reduce propeller noise remains a viable approach.

For a given propeller geometry, the noise footprint can greatly change with the operational conditions used, going as far as -10EPNLdB for a given procedure. Lowering the propeller efficiency by reducing the rotational speed gives access to low noise operations where propeller noise disappears under the airframe noise in this specific configuration. When noise reduction isn't required, rotational speed can be increased to operate at higher efficiency.

The computation of the REF's propeller has led to cumulative EPNL values lower than real recorded values for different ATR72 configurations. These underpredictions can be caused by several parameters. Among these, it is assumed that airframe noise model inaccuracies (due to the different architecture) and flight path/flight conditions inaccuracies account for most of the difference because the smallest discrepancy is obtained in takeoff where airframe noise isn't dominant, and conditions known with more certainties. Those uncertainties don't apply stricto sensu to the E9X because its architecture is closer to the type of aircraft used to build the airframe noise model and because the flight path and conditions are fixed by Elysian. With that in mind, the noise of the selected propeller design for the E9X appears to be in the range of the real ATR72, with the quietest operations 10EPNLdB below and the most efficient operations at the same level as the noisiest ATR72 configuration.

Acknowledgments

The research in this paper is founded by Elysian Aircraft company. The authors would like to thank Dr. Roberto Merino Martinez for his help and implication in all the discussions regarding noise perception and certification. G. Margalida and T. Sinnige declare that they don't have competing interests, and that they have performed this research in an objective way to the best of their ability. R. de Vries, J. Exalto and R. E. Wolleswinkel declare that they have competing interests, and that they have performed this research in an objective way to the best of their abilities.

References

[1] R. de Vries, R. E. Wolleswinkel, M. Hoogreef, and R. Vos, "A New Perspective on Battery-Electric Aviation, Part II: Conceptual Design of a 90-Seater," in *AIAA SCITECH 2024 Forum*, Reston, Virginia: American Institute of Aeronautics and Astronautics, Jan. 2024. doi: 10.2514/6.2024-1490.

[2] R. E. Wolleswinkel, R. de Vries, M. Hoogreef, and R. Vos, "A New Perspective on Battery-Electric Aviation, Part I: Reassessment of Achievable Range," in *AIAA SCITECH 2024 Forum*, Reston, Virginia: American Institute of Aeronautics and Astronautics, Jan. 2024. doi: 10.2514/6.2024-1489.

[3] W. Khan and M. Nahon, "Improvement and validation of a propeller slipstream model for small unmanned aerial vehicles," in *2014 International Conference on Unmanned Aircraft Systems (ICUAS)*, IEEE, May 2014, pp. 808–814. doi: 10.1109/ICUAS.2014.6842326.

[4] W. F. Phillips and D. O. Snyder, "Modern adaptation of Prandtl's classic lifting-line theory," *J Aircr*, vol. 37, no. 4, pp. 662–670, 2000, doi: 10.2514/2.2649.

[5] C. D. Goates and D. F. Hunsaker, “Practical Implementation of a General Numerical Lifting-Line Method,” in *AIAA Scitech 2021 Forum*, Reston, Virginia: American Institute of Aeronautics and Astronautics, Jan. 2021. doi: 10.2514/6.2021-0118.

[6] D. Küchemann, “A Simple Method for Calculating the Span and Chordwise Loading on Straight and Swept Wings of any Given Aspect Ratio at Subsonic Speeds.”

[7] J. Goyal, “Hanson’s Model in Frequency Domain - Tonal Noise of Rotors in Uniform Inflow.,” 2024, *4TU.ResearchData. software*: 1.

[8] D. B. Hanson, “Helicoidal Surface Theory for Harmonic Noise of Propellers in the Far Field,” vol. 18, no. 10, 1980.

[9] T. F. Brooks, D. Stuart, and M. A. Marcolini, “Airfoil Self-Noise and Prediction,” 1989.

[10] M. R. Fink, “Noise Component Method for Airframe Noise.”

[11] W. E. Zorumski, “Aircraft Noise Prediction Program Theoretical Manual.”

[12] J. Sodja, R. Drazumeric, T. Kosel, and P. Marzocca, “Design of Flexible Propellers with Optimized Load-Distribution Characteristics,” *J Aircr*, vol. 51, no. 1, pp. 117–128, Jan. 2014, doi: 10.2514/1.C032131.

[13] ICAO, “Annex 16 Environmental Protection, Volume 1 — Aircraft Noise.”